Theoretical calculation of the acoustic radiation force on layered cylinders in a plane standing wave—comparison of near- and far-field solutions

2006 J. Phys. A: Math. Gen. 39 6085

(http://iopscience.iop.org/0305-4470/39/20/031)

INSTITUTE OF PHYSICS PUBLISHING JOURNAL OF PHYSICS A: MATHEMATICAL AND GENERAL

J. Phys. A: Math. Gen. **39** (2006) 6085–6096 doi:10.1088/0305-4470/39/20/031

Theoretical calculation of the acoustic radiation force on layered cylinders in a plane standing wave—comparison of near- and far-field solutions

F G Mitri[1] **and Z E A Fellah**[2]

[1] Mayo Clinic College of Medicine, Department of Physiology and Biomedical Engineering, Ultrasound Research Laboratory, 200 First Street SW, Rochester MN 55905, USA
[2] Laboratoire de Mécanique et d'Acoustique, CNRS-UPR 7051, 31 chemin Joseph Aiguier, Marseille 13009, France

E-mail: mitri@ieee.org and mitri.farid@mayo.edu

Received 17 October 2005, in final form 7 March 2006
Published 3 May 2006
Online at stacks.iop.org/JPhysA/39/6085

Abstract

In this work, the theory for the acoustic radiation force on cylinders in a standing wave is extended to the case of cylinders coated with a viscoelastic polymer-type layer and immersed in ideal compressible fluids. Moreover, two different expressions for the radiation force function Y_{st} (which is the radiation force per unit cross-sectional surface and unit energy density) for elastic cylinders are compared. The first expression for the radiation force function is obtained on the basis of the *far-field* derivation approach; however, the second expression is obtained from the *near-field* solution. It is demonstrated that the computational differences are commensurate with the same result. In the second step, calculations for the radiation force function are performed for an elastic brass cylinder coated by a viscoelastic (sound absorptive) phenolic polymer layer for four thicknesses of the outer covering layer. Additional calculations are also performed to investigate the fluid-loading effect on the radiation force function curves. Some of the results for the radiation force can be relevant to the non-contact manipulation of coated tubular phantoms in space-related applications.

PACS numbers: 43.20.+g, 43.25.+y

1. Introduction

The fundamental problem related to the calculation of the acoustic radiation force on a rigid cylinder in both progressive and standing plane waves was reported in the early-published work of Awatani [1]. His derivation included a dipole ($n = 1$) term in the acoustic scattered field leading the cylinder to be movable. In that study, the radiation force was numerically

evaluated in a small range of dimensionless frequency ($0 \leqslant ka \leqslant 5$; k is the wave vector of the incident wave in the fluid medium, a is the cylinder's radius) based on a near-field derivation approach. Afterwards, Hasegawa *et al* [2] extended Awatani's work by including the effects of compressibility as well as the elastic vibrations of the cylinder only for the case of incident plane *progressive* or travelling waves. In the long sound wavelength limit (Rayleigh regime in which $ka \ll 1$), it was shown that the effect of elasticity can be ignored. However, deviations from Awatani's theory appeared for $ka \geqslant 2$ and gave rise to sharp maxima and minima related to the cylinder's resonance elastic vibrational modes. The case of elastic cylindrical and spherical shells in plane progressive waves was also examined [3] and extended to take into account compressional and shear waves' absorption inside the shells' materials [4, 5].

On the other hand, the study of the acoustic radiation force on cylinders in plane standing waves in non-viscous fluids gained a particular attention in muscle research to measure the tensile strength of a protein filament [6]. In that work, Wu *et al* [6] gave a long-wavelength approximation for the radiation force on a rigid circular cylinder (protein filament) for the situation where the cylinder's axis was constrained to be parallel to the equi-amplitude surfaces of a plane standing wave. Their derivation was limited to include a quadrupole ($n = 2$) term in the acoustic scattered field. However, it is anticipated that the truncation of the series will lead to significant errors when their derivation is compared with more complete solutions. In a recent work [7], approximate calculations of the radiation force on small moveable and immovable cylinders in plane standing waves in non-viscous fluids have been carried out in the limit $ka \ll kh$ (h is the distance in the x-direction from the nearest pressure antinode to the centre of the cylinder), in which a quadrupole ($n = 2$) term was included in the acoustic scattered field as well.

The study of the radiation force on cylinders in plane standing waves has also found another application in fluid dynamic research. One of the interests in this problem was motivated by the essential need to understand the Rayleigh–Plateau capillary instabilities exhibited by long liquid bridges [8–10]. Moreover, in microgravity environment provided by Space flights, intense interest has arisen in non-contact and non-destructive measurement of materials' physical properties, especially for the container-less processing of elongated tubular specimens in acoustic levitation applications [11, 12].

Recently, the acoustic radiation force on rigid immovable, elastic and viscoelastic cylinders [13] and shells [14, 15] immersed in non-viscous fluids in plane stationary and quasistationary waves is theoretically studied, based on the integration of the time-averaged momentum flux tensor over the equilibrium surface of the circular cylinder (near-field derivation approach). In that work, the radiation force function formulation is simplified mathematically and improved into a more general form in view of the other existing expressions. The radiation force function, which is the radiation force per unit energy density and unit cross-sectional surface of the cylinder, is plotted versus the dimensionless frequency for various materials. On the other hand, Wei *et al* [16] have deduced another formula for the radiation force function in a perfect standing wave. According to their method, the force is calculated from the far-field acoustic scattering. This method was previously used to calculate the acoustic radiation force on small spheres and bubbles [17–19].

The two approaches mentioned above must lead to the same result. Differences, however, exist with respect to the analytical expressions. The present paper is an attempt to investigate the above-mentioned problem based on numerical analyses. Moreover, the theory is extended here to the case of cylinders coated by a viscoelastic layer of polymer-type material and placed in a plane stationary or standing wave. It is particularly interesting to study the radiation force on coated tubular (elastic or viscoelastic) specimens in non-contact and non-destructive procedures for space-related applications, since these processes usually concern

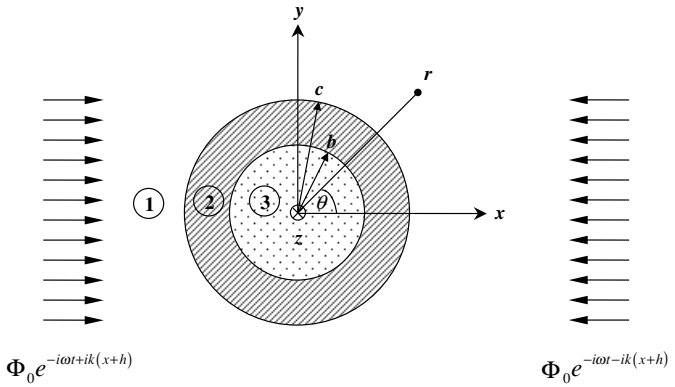

Figure 1. Geometry of the layered cylinder placed in a standing plane-wave field. Media 1, 2 and 3 correspond to the exterior fluid, coating layer and solid core materials, respectively.

the manipulation of core media within coated objects. The theory gives *a priori* information on the magnitude of the force used to manipulate or levitate coated cylindrical specimens in a low-gravity environment. Additional numerical calculations for the radiation force function are performed for a brass elastic cylinder coated by a viscoelastic phenolic polymer layer for four thicknesses of the outer covering. Furthermore, the fluid-loading effect on the radiation force function curves is analysed as well by considering a high-density fluid surrounding the layered cylinders.

2. Method

For layered cylinders, the exact evaluation of the radiation force involves the complete solution of the associated acoustic scattering problem. Hence, the acoustic scattering problem should be solved first. The radiation force is then determined by integrating the time-averaged momentum-flux tensor over the equilibrium surface of the cylinder in an ideal fluid.

2.1. Determination of the total velocity potential in terms of cylindrical wavefunctions

The geometry and the coordinate system used are shown in figure 1. The centre of the layered cylinder coincides with the origin of a rectangular coordinate system, and the plane waves approach the cylinder along the positive and negative x-axes ($\theta = 0$ and π, respectively).

The Helmholtz equation describing the wave propagation in the medium is given by

$$\left(\nabla^2 + k_1^2\right)\varphi_1 = 0, \tag{1}$$

where the compressional wave number in the exterior fluid (medium 1) is $k_1 = \omega/c_1$.

The time-independent *total* scalar velocity potential in a *standing wave* field (solution of equation (1)) is the sum of the incident and scattered fields that can be expressed in cylindrical coordinates by [13]

$$\varphi_1(r,\theta) = \sum_{n=0}^{\infty} \Lambda_{n,1}\varepsilon_n i^n \left(J_n(k_1 r) + a_n H_n^{(1)}(k_1 r)\right)\cos(n\theta), \tag{2}$$

where $\Lambda_{n,1} = \Phi_0\{e^{ik_1 h} + (-1)^n\, e^{-ik_1 h}\}$, Φ_0 is the amplitude, h is the distance in the x-direction from the nearest pressure antinode to the centre of the cylinder, ε_n is the Neumann factor

which is defined by $\varepsilon_0 = 1$, and $\varepsilon_j = 2$, $j = 1, \ldots, n$, $J_n(\cdot)$ and $H_n^{(1)}(\cdot)$ are the cylindrical Bessel and Hankel functions of the first kind of order n, respectively, and a_n are the unknown scattering coefficients that will be determined by the appropriate boundary conditions.

The waves inside the layered cylinder (media 2 and 3) are represented by suitable solutions of the Helmholtz equations:

$$\left(\nabla^2 + k_{L,2,3}^2\right)\Phi_{2,3} = 0, \tag{3}$$

$$\left(\nabla^2 + k_{S,2,3}^2\right)\Psi_{2,3} = 0, \tag{4}$$

where

$$k_{L,2,3} = \frac{\omega}{[(\lambda_{2,3} + 2\mu_{2,3})/\rho_{2,3}]^{1/2}}, \qquad \text{and} \qquad k_{S,2,3} = \frac{\omega}{[\mu_{2,3}/\rho_{2,3}]^{1/2}},$$

refer to the longitudinal and shear wave numbers in the solid media, respectively.

Similarly, the longitudinal and shear waves inside the layer (medium 2) are represented in cylindrical coordinates by

$$\Phi_2(r,\theta) = \sum_{n=0}^{\infty} \Lambda_{n,L,2}\varepsilon_n i^n \left(b_n J_n(k_{L,2}r) + c_n Y_n(k_{L,2}r)\right)\cos(n\theta), \tag{5}$$

$$\Psi_2(r,\theta) = \sum_{n=0}^{\infty} \Lambda_{n,S,2}\varepsilon_n i^n \left(d_n J_n(k_{S,2}r) + e_n Y_n(k_{S,2}r)\right)\sin(n\theta), \tag{6}$$

where $Y_n(\cdot)$ are the cylindrical Bessel functions of the second kind. Sound absorption by the viscoelastic layer is customarily modelled by introducing complex size parameters (or wave numbers, respectively), accounting for losses inside the covering layer. Incorporating complex wave numbers into the acoustic scattering theory holds only for linear viscoelasticity [20–24].

In the core material (medium 3), the potentials solution of equations (3) and (4) are given by

$$\Phi_3(r,\theta) = \sum_{n=0}^{\infty} \Lambda_{n,L,3}\varepsilon_n i^n f_n J_n(k_{L,3}r)\cos(n\theta), \tag{7}$$

$$\Psi_3(r,\theta) = \sum_{n=0}^{\infty} \Lambda_{n,S,3}\varepsilon_n i^n g_n J_n(k_{S,3}r)\sin(n\theta). \tag{8}$$

The parameters, a_n, b_n, c_n, d_n, e_n, f_n and g_n, are the unknown coefficients determined from the following boundary conditions:

- At the outside boundary of the coated cylinder (interface at media 1 and 2), the displacements (velocities) and normal stresses must be continuous and the tangential stresses must be zero, leading to
- $v_r^{(1)}\big|_{r=c} = -\mathrm{i}\omega U_r^{(2)}\big|_{r=c}$;
- $\sigma_{rr}^{(1)}\big|_{r=c} = \sigma_{rr}^{(2)}\big|_{r=c}$;
- $\sigma_{r\theta}^{(2)}\big|_{r=c} = 0$.
- At the interface between the outer layer and core material (interface at media 2 and 3), the radial and tangential displacements are continuous, and the radial and tangential stresses of adjoining materials are equal:
- $U_r^{(2)}\big|_{r=b} = U_r^{(3)}\big|_{r=b}$;
- $U_\theta^{(2)}\big|_{r=b} = U_\theta^{(3)}\big|_{r=b}$;
- $\sigma_{rr}^{(2)}\big|_{r=b} = \sigma_{rr}^{(3)}\big|_{r=b}$;
- $\sigma_{r\theta}^{(2)}\big|_{r=b} = \sigma_{r\theta}^{(3)}\big|_{r=b}$.

The detailed expressions of the velocities, displacements and stress components are given in appendix A.

The boundary conditions lead to seven linear equations with seven (scattering) coefficients. The general solution for a_n is given by

$$a_n = \frac{\begin{vmatrix} \lambda_1^* & \lambda_{12} & \lambda_{13} & \lambda_{14} & \lambda_{15} & 0 & 0 \\ \lambda_2^* & \lambda_{22} & \lambda_{23} & \lambda_{24} & \lambda_{25} & 0 & 0 \\ 0 & \lambda_{32} & \lambda_{33} & \lambda_{34} & \lambda_{35} & 0 & 0 \\ 0 & \lambda_{42} & \lambda_{43} & \lambda_{44} & \lambda_{45} & \lambda_{46} & \lambda_{47} \\ 0 & \lambda_{52} & \lambda_{53} & \lambda_{54} & \lambda_{55} & \lambda_{56} & \lambda_{57} \\ 0 & \lambda_{62} & \lambda_{63} & \lambda_{64} & \lambda_{65} & \lambda_{66} & \lambda_{67} \\ 0 & \lambda_{72} & \lambda_{73} & \lambda_{74} & \lambda_{75} & \lambda_{76} & \lambda_{77} \end{vmatrix}}{\begin{vmatrix} \lambda_{11} & \lambda_{12} & \lambda_{13} & \lambda_{14} & \lambda_{15} & 0 & 0 \\ \lambda_{21} & \lambda_{22} & \lambda_{23} & \lambda_{24} & \lambda_{25} & 0 & 0 \\ 0 & \lambda_{32} & \lambda_{33} & \lambda_{34} & \lambda_{35} & 0 & 0 \\ 0 & \lambda_{42} & \lambda_{43} & \lambda_{44} & \lambda_{45} & \lambda_{46} & \lambda_{47} \\ 0 & \lambda_{52} & \lambda_{53} & \lambda_{54} & \lambda_{55} & \lambda_{56} & \lambda_{57} \\ 0 & \lambda_{62} & \lambda_{63} & \lambda_{64} & \lambda_{65} & \lambda_{66} & \lambda_{67} \\ 0 & \lambda_{72} & \lambda_{73} & \lambda_{74} & \lambda_{75} & \lambda_{76} & \lambda_{77} \end{vmatrix}}, \tag{9}$$

where λ_1^*, λ_2^* and λ_{ij} are the dimensionless elements of the determinants given in appendix B. The coefficient is a complex number which can be written as $a_n = \alpha_n + \mathrm{i}\beta_n$.

2.2. *Acoustic radiation force on a layered cylinder–comparison of two solutions*

Wei *et al* [16] have developed a solution for the radiation force function for cylinders in a standing wave, based on the far-field acoustic scattered field. According to their theory,

$$Y_{\mathrm{st}}^{\text{far-field}} = \frac{4}{k_1 c} \sum_{n=0}^{N\to\infty} (-1)^{n+1} [\varepsilon_n \beta_n + 2(\alpha_{n+1}\beta_n - \alpha_n \beta_{n+1})], \tag{10}$$

where α_n and β_n are real and imaginary parts of the scattering coefficients a_n defined by equation (9).

On the other hand, the solution developed in [13] gives the following expression for the radiation force function for cylinders in a standing wave:

$$Y_{\mathrm{st}}^{\text{near-field}} = \frac{4}{k_1 c} \sum_{n=0}^{N\to\infty} (-1)^{n+1} [(1 + 2\alpha_{n+1})\beta_n - (1 + 2\alpha_n)\beta_{n+1}]. \tag{11}$$

Following the method previously developed in [25], the nth terms on the right-hand sides of equations (10) and (11) were evaluated numerically:

$$Y_N^{\text{far-field}} = \frac{4}{k_1 c} (-1)^{n+1} [\varepsilon_n \beta_n + 2(\alpha_{n+1}\beta_n - \alpha_n \beta_{n+1})], \tag{12}$$

and

$$Y_N^{\text{near-field}} = \frac{4}{k_1 c} (-1)^{n+1} [(1 + 2\alpha_{n+1})\beta_n - (1 + 2\alpha_n)\beta_{n+1}]. \tag{13}$$

As an example of this comparison, a stainless steel cylinder suspended in a plane standing wave in water is considered. The mechanical properties of this material used in the calculations are listed in table 1. It is also crucial to extend the maximum index N (= 40 for this example)

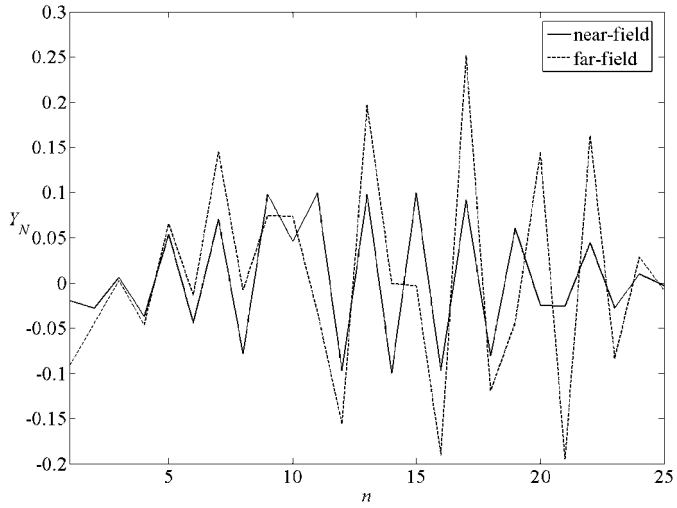

Figure 2. Values of the functions $Y_N^{\text{far-field}}$ and $Y_N^{\text{near-field}}$ given by equations (12) and (13) versus n, for a stainless steel cylinder without coating ($e_1 = 1$) for $k_1 c = 20$.

Table 1. Material parameters used in the numerical calculations.

Material	Mass density (10^3 kg m^{-3})	Compressional velocity (m s^{-1})	Shear velocity (m s^{-1})	Normalized longitudinal absorption γ_{21}	Normalized shear absorption γ_{22}
Brass	8.1	3830	2050	–	–
Phenolic polymer	1.22	2840	1320	0.0119	0.0257
Mercury	13.6	1407	–	–	–
Water	1.00	1500	–	–	–

to exceed $k_1 c$ to ensure proper convergence. According to the theory developed in [13] the corresponding value of Y_{st} is 0.1205 at $k_1 c = 20$.

Equations (12) and (13) are plotted versus n in figure 2. As seen in this figure, one can obviously observe the great difference between the two plots. This makes serious doubt about the agreement between the two theories since Wei *et al* [16] anticipated the equivalence that should exist between the near and far-field solutions. However, in point of fact, it is the sum of $Y_N^{\text{far-field}}$ or $Y_N^{\text{near-field}}$ for all n, but not the nth term itself that should be evaluated. Therefore, summing up $Y_N^{\text{far-field}}$ or $Y_N^{\text{near-field}}$ for all values of n, we obtain the same value of 0.1205 as Y_{st} values of both theories, for $k_1 c = 20$. Therefore, it is suggested that the two solutions are numerically equivalent in spite of the apparent discrepancy. This is explained as follows: if we denote by Δ_N the difference between the partial sums up to $n = N$ in equations (12) and (13) we obtain

$$\begin{aligned}\Delta_N &= \sum_{n=0}^{N} \left(Y_N^{\text{far-field}} - Y_N^{\text{near-field}}\right), \\ &= \frac{8}{k_1 c} \sum_{n=0}^{N} (-1)^{n+1} [\beta_n (\varepsilon_n - 1) + \beta_{n+1}], \\ &= \frac{8}{k_1 c} (-1)^{N+1} \beta_{N+1}.\end{aligned} \tag{14}$$

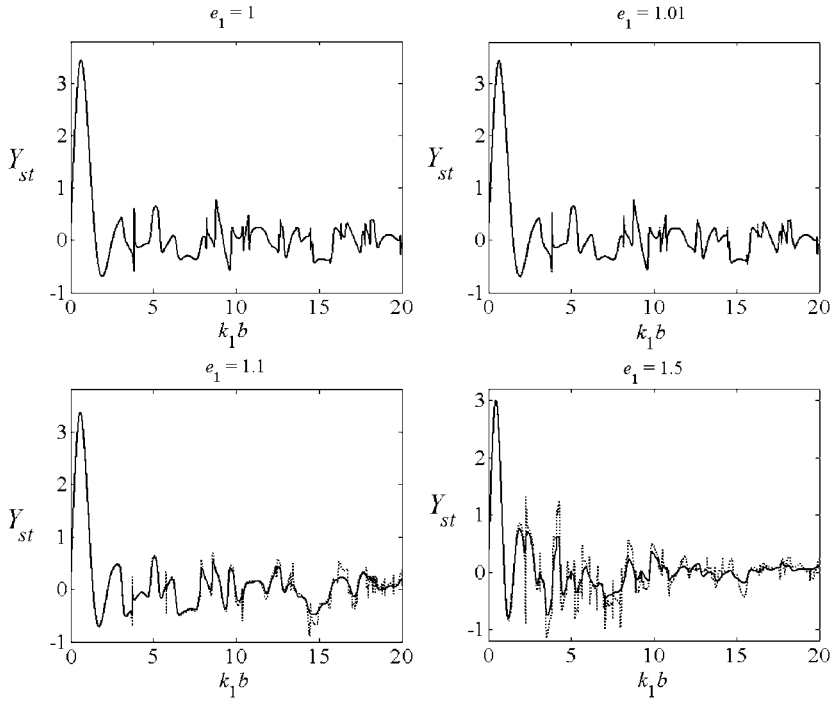

Figure 3. Y_{st} curves for a coated brass cylinder immersed in water for four thicknesses of the coating viscoelastic layer, with (solid line) and without (dashed line) absorption. The coating material is chosen to be phenolic polymer. Note that $e_1 = 1$ corresponds to the case of an uncoated cylinder.

It can be numerically proved that β_{N+1} is at most a small quantity so long as equation (10) or (11) is convergent. Hence, $\lim_{N\to\infty} \Delta_N = 0$, and the two solutions, i.e. equations (10) and (11) are numerically equivalent.

3. Numerical results and discussion

The objective here is to show a few numerical calculations of the radiation force function for standing waves for coated cylinders immersed in water and mercury, respectively, using equation (11) as a function the size parameter $x = k_1 b$. Both core and layer materials could be absorbent; however, in our case, the outer layer consists of phenolic polymer; a viscoelastic material, and the core material of brass material that is considered to be elastic and loss-less. These types of materials are chosen as an example to illustrate the theory. The mechanical parameters for these materials used in the calculations are given in table 1. Absorption of sound inside the outer layer is included by introducing complex size parameters in the theory (see appendix B). The normalized absorption coefficients for both compressional and shear waves are listed in table 1. The thickness of the viscoelastic layer is $e_1 = c/b$ (figure 1).

Radiation force function curves are plotted with particular emphasis on the effect of absorption and the thickness of the outer covering by varying the parameter e_1. Computations for brass cylinders are performed in a large range of dimensionless frequency $0 \leqslant x \leqslant 20$ by

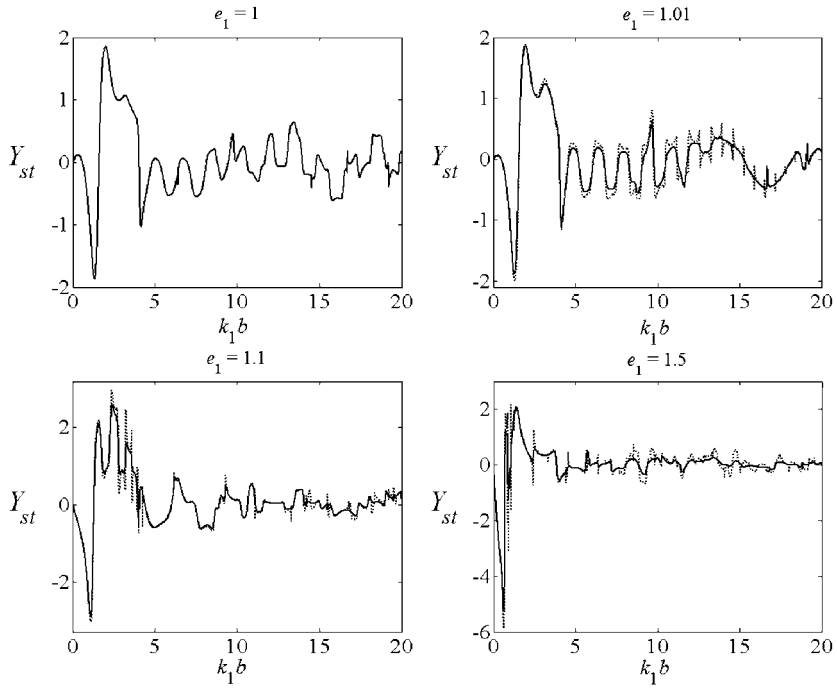

Figure 4. $Y_{\rm st}$ curves for a coated brass cylinder immersed in mercury with (solid line) and without (dashed line) absorption. It is obvious that increasing the layer thickness for small $k_1 b$ values causes the radiation force to be more attractive ($Y_{\rm st}^{e_1=1.5}|_{k_1 b=0.65} < Y_{\rm st}^{e_1=1.1}|_{k_1 b=1.1} < Y_{\rm st}^{e_1=1.01}|_{k_1 b=1.29}$).

intervals of 0.001. It is very important to choose a sufficiently small sampling step to allow capturing the resonance peaks that are very sharp. One hundred fifty terms are kept in the sum (i.e. equation (11)) used to generate the $Y_{\rm st}$ curves to insure proper convergence of the series.

According to the model previously developed in [13], the force-per-length is expressed as

$$F_{\rm x} = Y_{\rm st} S_{\rm c} E_{\rm p} \sin(2k_1 h), \tag{15}$$

where $S_{\rm c}$ is the cross-sectional surface for a unit-length cylinder, and $E_{\rm p}$ is the mean energy density for plane progressive waves. Thus, the radiation force vanishes for $k_1 h = \pm\frac{n\pi}{2}$. If the cylinder is centred on a pressure antinode, $n = 0$, and if it is centred or on a pressure node, $n = 1, 2, \ldots$. The magnitude of the radiation force is maximum when the cylinder is at the intermediate location determined by $k_1 h = \pm(2n + 1)\frac{\pi}{4}$; $n = 0, 1, \ldots$. Moreover, when $Y_{\rm st} > 0$, the radiation force is repulsive and pushes the cylinder towards a pressure node, and when $Y_{\rm st} > 0$, the radiation force is attractive and pushes the cylinder towards a pressure antinode.

Figure 3 shows the radiation force function for a layered cylinder immersed in water with and without taking absorption into account inside the outer covering layer, for four layer thicknesses. At low $k_1 b$ values, one notes that the radiation force is repulsive ($Y_{\rm st} > 0$). The radiation force function for $e_1 = 1$ corresponds to a cylinder without coating. Since each of the plots is the sum of many (i.e. 150) partial-waves or normal modes, which interfere one with the other in a sensitive way, $Y_{\rm st}$ exhibits many rapid oscillations, peaks and dips which are due to resonances excited in the cylinder as well as in the coating layer by the incident

field. Undoubtedly, the effect of increasing the absorbing outer covering layer thickness has a prominent effect in damping and shifting the resonance peaks of the Y_{st} curves.

The case of a brass cylinder coated by a phenolic polymer layer immersed in mercury is an example of a situation where the fluid-loading has a significant effect on the radiation force. Figure 4 shows the variations of the Y_{st} curves with and without absorption in the covering layer. In figure 4, we note that increasing the layer thickness at low k_1b values decreases Y_{st} with and without including the effect of absorption within the coating layer. Therefore, the radiation force becomes more attractive when the layer thickness increases. Moreover, the fluid-loading produces interactions between various resonance modes, which is especially observed in the bandwidth $5 \leqslant x = k_1b \leqslant 15$ for $e_1 = 1.01$; a series of successive resonance peaks tend to appear which correspond to the coupled vibrations of the cylinder and the viscoelastic layer. When the surrounding fluid medium changes from water to mercury, the resonance peak (maximum), observed at low k_1b values in figure 3, is transformed into a minimum (figure 4) and shifts to low k_1b values as the thickness of the outer covering layer increases.

4. Conclusion

In this paper, the theory for the acoustic radiation force in a standing plane wave is extended to the case of layered cylinders. Particular attention is directed towards sound absorption inside the viscoelastic layer and its effect on the radiation force function curves. By varying the coating layer thickness, additional resonance modes are excited which appear as a series of maxima and minima peaks in the radiation force function curves. As of the result of increasing the fluid-loading and the thickness of the outer covering layer, the radiation force becomes more attractive at low k_1b values. These numerical computations show that the results previously obtained for cylinders [13] and cylindrical shells [15] can be reproduced by varying the core and layered media' mechanical parameters. Moreover, it is demonstrated that the expressions for the radiation force functions in the near- and far-field derivation approaches are equivalent and give the same result.

After this manuscript had been submitted for publication, another paper on the equivalence of near- and far-field solutions appeared in JASA [26]. The authors of [26] showed that using an appropriate grouping of terms, the radiation force function Y_{st} for cylinders in a plane standing wave based on far-field acoustic scattering [16] is transformed to the expression given by equation (11) and published previously in [13, 15]. There is an excellent qualitative and quantitative agreement between the demonstration in section 2.2 of this present paper and their approach.

Appendix A. Field equations

The basic field equations in cylindrical coordinates are given as follows; the velocity component of the wave in the exterior fluid medium is $v_r^{(1)} = -\frac{\partial \varphi_1}{\partial r}$, where φ_1 is given by equation (7).

Similarly, the displacements expressed in terms of potentials in the layered cylinder are

$$U_r^{(2,3)} = \frac{\partial \Phi_{2,3}}{\partial r} + \frac{1}{r}\frac{\partial \Psi_{2,3}}{\partial \theta}, \qquad U_\theta^{(2,3)} = \frac{1}{r}\frac{\partial \Phi_{2,3}}{\partial \theta} - \frac{\partial \Psi_{2,3}}{\partial r},$$

where $\Phi_{2,3}$ and $\mathbf{\Psi}_{2,3}(0, 0, \Psi_{2,3})$ are the scalar and vector potentials, with their components given in equations (5)–(8).

The stress component in the exterior fluid is $\sigma_{rr}^{(1)} = \mathrm{i}\omega\rho_1\varphi_1$, where ρ_1 is the exterior fluid mass density, and the stresses components in the layered cylinder are

$$\sigma_{rr}^{(2,3)} = 2\mu_{2,3}\frac{\partial U_r^{(2,3)}}{\partial r} + \lambda_{2,3}(\nabla \cdot \mathbf{U}_{2,3}),$$
$$\sigma_{r\theta}^{(2,3)} = \mu_{2,3}\left(\frac{1}{r}\frac{\partial U_r^{(2,3)}}{\partial \theta} + r\frac{\partial}{\partial r}\left(\frac{U_\theta^{(2,3)}}{r}\right)\right) = \mu_{2,3}\left(\frac{1}{r}\frac{\partial U_r^{(2,3)}}{\partial \theta} + \frac{\partial U_\theta^{(2,3)}}{\partial r} - \frac{U_\theta^{(2,3)}}{r}\right),$$

where $\lambda_{2,3}$ and $\mu_{2,3}$ are the Lamé coefficients and $\mathbf{U}_{2,3} = \boldsymbol{\nabla}\Phi_{2,3} + (\boldsymbol{\nabla} \times \boldsymbol{\Psi}_{2,3})$ is the vector displacement.

Appendix B. Matrix elements

The parameters ρ_1 and ρ_2 are the mass densities of the fluid surrounding the cylinder and the viscoelastic coating, respectively. The parameters $e_1 = c/b$; where c and b are the outer and inner radii (figure 1), $x = k_1 b$; where $k_1 = \frac{\omega}{c_1}$ and c_1 is the sound velocity in the fluid medium, $\tilde{x}_{21} = x\frac{c_1}{c_{21}}(1 + \mathrm{i}\gamma_{21})$ and $\tilde{x}_{22} = x\frac{c_1}{c_{22}}(1 + \mathrm{i}\gamma_{22})$ where c_{21} and c_{22} are the compressional and shear sound velocities in the viscoelastic layer and γ_{21} and γ_{22} are their corresponding absorption coefficients (table 1), respectively, $x_{31} = x\frac{c_1}{c_{31}}$ and $x_{32} = x\frac{c_1}{c_{32}}$ where c_{31} and c_{32} are the compressional and shear sound velocities in the core material, respectively. $y_1 = xe_1$, $\tilde{y}_{21} = \tilde{x}_{21}e_1$, $\tilde{y}_{22} = \tilde{x}_{22}e_1$, $y_{31} = x_{31}e_1$, $y_{32} = x_{32}e_1$ and $\Lambda_{23} = \frac{\rho_2}{\rho_3}\left(\frac{c_{22}}{c_{32}}\right)^2$, where ρ_3 is the core material mass density.

The following terms are the expressions for the elements of determinants appearing in equation (9).

$$\lambda_{11} = \frac{\rho_1}{\rho_2}\tilde{y}_{22}^2 H_n^{(1)}(y_1),$$
$$\lambda_{12} = \left(2n^2 - \tilde{y}_{22}^2\right)J_n(\tilde{y}_{21}) - 2\tilde{y}_{21}J_n'(\tilde{y}_{21}),$$
$$\lambda_{13} = \left(2n^2 - \tilde{y}_{22}^2\right)Y_n(\tilde{y}_{21}) - 2\tilde{y}_{21}Y_n'(\tilde{y}_{21}),$$
$$\lambda_{14} = 2n(\tilde{y}_{22}J_n'(\tilde{y}_{22}) - J_n(\tilde{y}_{22})),$$
$$\lambda_{15} = 2n(\tilde{y}_{22}Y_n')((\tilde{y}_{22}) - Y_n(\tilde{y}_{22})),$$
$$\lambda_{21} = -y_1 H_n^{(1)'}(y_1),$$
$$\lambda_{22} = \tilde{y}_{21}J_n'(\tilde{y}_{21}),$$
$$\lambda_{23} = \tilde{y}_{21}Y_n'(\tilde{y}_{21}),$$
$$\lambda_{24} = nJ_n(\tilde{y}_{22}),$$
$$\lambda_{25} = nY_n(\tilde{y}_{22}),$$
$$\lambda_{32} = 2n(J_n(\tilde{y}_{21}) - \tilde{y}_{21}J_n'(\tilde{y}_{21})),$$
$$\lambda_{33} = 2n(Y_n(\tilde{y}_{21}) - \tilde{y}_{21}Y_n'(\tilde{y}_{21})),$$
$$\lambda_{34} = 2\tilde{y}_{22}J_n'(\tilde{y}_{22}) - \left(2n^2 - \tilde{y}_{22}^2\right)J_n(\tilde{y}_{22}),$$
$$\lambda_{35} = 2\tilde{y}_{22}Y_n'(\tilde{y}_{22}) - \left(2n^2 - \tilde{y}_{22}^2\right)Y_n(\tilde{y}_{22}),$$
$$\lambda_{42} = \tilde{x}_{21}J_n'(\tilde{x}_{21}),$$
$$\lambda_{43} = \tilde{x}_{21}Y_n'(\tilde{x}_{21}),$$
$$\lambda_{44} = nJ_n(\tilde{x}_{22}),$$
$$\lambda_{45} = nY_n(\tilde{x}_{22}),$$
$$\lambda_{46} = -x_{31}J_n'(x_{31}),$$

$$
\begin{aligned}
\lambda_{47} &= -nJ_n(x_{32}),\\
\lambda_{52} &= -nJ_n(\tilde{x}_{21}),\\
\lambda_{53} &= -nY_n(\tilde{x}_{21}),\\
\lambda_{54} &= -\tilde{x}_{22}J_n'(\tilde{x}_{22}),\\
\lambda_{55} &= -\tilde{x}_{22}Y_n'(\tilde{x}_{22}),\\
\lambda_{56} &= nJ_n(x_{31}),\\
\lambda_{57} &= x_{32}J_n'(x_{32}),\\
\lambda_{62} &= \Lambda_{23}\left(\left(2n^2-\tilde{x}_{22}^2\right)J_n(\tilde{x}_{21})-2\tilde{x}_{21}J_n'(\tilde{x}_{21})\right),\\
\lambda_{63} &= \Lambda_{23}\left(\left(2n^2-\tilde{x}_{22}^2\right)Y_n(\tilde{x}_{21})-2\tilde{x}_{21}Y_n'(\tilde{x}_{21})\right),\\
\lambda_{64} &= 2n\Lambda_{23}(\tilde{x}_{22}J_n'(\tilde{x}_{22})-J_n(\tilde{x}_{22})),\\
\lambda_{65} &= 2n\Lambda_{23}(\tilde{x}_{22}Y_n'(\tilde{x}_{22})-Y_n(\tilde{x}_{22})),\\
\lambda_{66} &= 2x_{31}J_n'(x_{31})-\left(2n^2-x_{32}^2\right)J_n(x_{31}),\\
\lambda_{67} &= 2n(J_n(x_{32})-x_{32}J_n'(x_{32})),\\
\lambda_{72} &= 2n(J_n(\tilde{x}_{21})-\tilde{x}_{21}J_n'(\tilde{x}_{21})),\\
\lambda_{73} &= 2n(Y_n(\tilde{x}_{21})-\tilde{x}_{21}Y_n'(\tilde{x}_{21})),\\
\lambda_{74} &= 2\tilde{x}_{22}J_n'(\tilde{x}_{22})-\left(2n^2-\tilde{x}_{22}^2\right)J_n(\tilde{x}_{22}),\\
\lambda_{75} &= 2\tilde{x}_{22}Y_n'(\tilde{x}_{22})-\left(2n^2-\tilde{x}_{22}^2\right)Y_n(\tilde{x}_{22}),\\
\lambda_{76} &= \frac{2n}{\Lambda_{23}}(x_{31}J_n'(x_{31})-J_n(x_{31})),\\
\lambda_{77} &= \frac{1}{\Lambda_{23}}\left(\left(2n^2-x_{32}^2\right)J_n(x_{32})-2x_{32}J_n'(x_{32})\right),\\
\lambda_1^* &= -\frac{\rho_1}{\rho_2}\tilde{y}_{22}^2J_n(y_1),\\
\lambda_2^* &= y_1J_n'(y_1).
\end{aligned}
$$

References

[1] Awatani J 1955 *Mem. Inst. Sci. Ind. Osaka Univ.* **12** 95
[2] Hasegawa T, Saka K, Inoue N and Matsuzawa K 1988 *J. Acoust. Soc. Am.* **83** 1770
See also Mitri F G 2006 *New J. Phys.* in press
[3] Hasegawa T, Hino Y, Annou A, Noda H and Kato M 1993 *J. Acoust. Soc. Am.* **93** 154
[4] Mitri F G 2005 *Ultrasonics* **43** 271
[5] Mitri F G 2005 *Wave Motion* **43** 12
[6] Wu J, Du G, Work S S and Warshaw D 1990 *J. Acoust. Soc. Am.* **87** 581
[7] Haydock D 2005 *J. Phys. A: Math. Gen.* **38** 3279
[8] Marr-Lyon M J, Thiessen D B and Marston P L 1997 *J. Fluid Mech.* **351** 345
[9] Marr-Lyon M J, Thiessen D B and Marston P L 2001 *Phys. Rev. Lett.* **86** 2293
Marr-Lyon M J, Thiessen D B and Marston P L 2001 *Phys. Rev. Lett.* **87** 209901 (erratum)
[10] Marston P L and Thiessen D B 2004 *Ann. NY Acad. Sci.* **1027** 414
[11] Trinh E H 1985 *Rev. Sci. Instrum.* **56** 2059
[12] Ohsaka K, Rednikov A, Sadhal S S and Trinh E H 2002 *Rev. Sci. Instrum.* **73** 2091
[13] Mitri F G 2005 *Eur. Phys. J.* B **44** 71
[14] Mitri F G 2005 *Ultrasonics* **43** 681
[15] Mitri F G 2005 *J. Phys. A: Math. Gen.* **38** 9395
[16] Wei W, Thiessen D B and Marston P L 2004 *J. Acoust. Soc. Am.* **116** 201
Wei W, Thiessen D B and Marston P L 2005 *J. Acoust. Soc. Am.* **118** 551 (erratum)

[17] Gor'kov L P 1962 *Sov. Phys. Dokl.* **6** 773 (A typeset error has occurred in equation (8); the term '$\overline{v_{in}v_{in}}$' should be corrected as '$\overline{v_{in}v_{sc}}$')
[18] Löfstedt R and Putterman S 1991 *J. Acoust. Soc. Am.* **90** 2027
[19] Lee C P and Wang T G 1993 *J. Acoust. Soc. Am.* **93** 1637
[20] Hartmann B and Jarzynski J 1972 *J. Appl. Phys.* **43** 4304
[21] Vogt R H, Flax L, Dragonette L R and Neubauer W G 1975 *J. Acoust. Soc. Am.* **57** 558
Vogt R H, Flax L, Dragonette L R and Neubauer W G 1975 *J. Acoust. Soc. Am.* **62** 1315 (erratum)
[22] Hasegawa T, Kitagawa Y and Watanabe Y 1977 *J. Acoust. Soc. Am.* **62** 1298
[23] Hipp A K, Adjadj L P, Storti G and Morbidelli M 2002 *J. Acoust. Soc. Am.* **111** 1549
[24] Mitri F G 2005 *J. Sound. Vib.* **284** 494
[25] Hasegawa T 1977 *J. Acoust. Soc. Am.* **61** 1445
[26] Wei W and Marston P L 2005 *J. Acoust. Soc. Am.* **118** 3397